Radboud Repository

Radboud University Nijmegen

PDF hosted at the Radboud Repository of the Radboud University Nijmegen

The following full text is a publisher's version.

For additional information about this publication click this link.
http://hdl.handle.net/2066/98806

The Zeeman effect in the (0,0) band of the $A\ ^7\Pi - X\ ^7\Sigma^+$ transition of manganese monohydride, MnH

Timothy C. Steimle,[1,a)] Hailing Wang,[1] Jamie J. Gengler,[1] Michael Stoll,[2] and Gerard Meijer[2]

[1]*Department of Chemistry and Biochemistry, Arizona State University, Tempe, Arizona 85287-1604, USA*
[2]*Fritz-Haber-Institut der Max-Planck-Gesellschaft, Faradayweg 4-614195 Berlin, Germany*

The Zeeman tuning of the $P_1(0)$ line ($\nu = 17\,568.35$ cm^{-1}) of the $A\ ^7\Pi - X\ ^7\Sigma^+$ (0,0) band of manganese monohydride, MnH, has been investigated. The laser induced fluorescence spectrum of a supersonic molecular beam sample was recorded at a resolution of approximately 40 MHz and with field strengths of up to 362.0 mT. The observed spectrum was successfully fitted using a traditional effective Zeeman Hamiltonian to determine an effective magnetic g-factor for the $J = 2$ level of the F_1-spin component of the $A\ ^7\Pi(v=0)$ state. Spectral predictions of the $P_1(0)$ line at field strengths used in magnetic trapping experiments are presented. © 2008 American Institute of Physics. [DOI: 10.1063/1.3000007]

I. INTRODUCTION

The large magnetic moment-to-mass ratio of the first row transition metal monohydrides makes these molecules well suited for magnetic trapping.[1,2] Chromium monohydride, CrH, and manganese monohydride, MnH, are particularly favorable cases because the bonding mechanism produces ground electronic states of very high multiplicity.[3] In the case of CrH, the unpaired electron in the 4s orbital of the ground $^7S(sd^5)$ state of Cr directly forms a σ-type bond with the H 1s orbital, and the other five electrons in the d orbitals remain high-spin coupled to produce the $X\ ^6\Sigma^+$ state. In the case of MnH, the 4s orbital of the ground $^6S(s^2d^5)$ state of Mn first hybridizes by mixing with the $4p4s3d^5$ configuration prior to σ-type bond formation. The remaining sole electron in the $4s/4p$ σ-type antibonding hybrid orbital is high-spin coupled with the other five high-spin coupled electrons in the 3d orbitals to produce the $X\ ^7\Sigma^+$ state of MnH,

$$(4s/4p + 1s, \sigma)^2(3d\sigma)^1(3d\delta)^2(3d\pi)^2(4s/4p, \sigma)^1 \rightarrow X\ ^7\Sigma^+. \quad (1)$$

Ignoring nuclear spin effects and assuming that the $X\ ^6\Sigma^+$ and $X\ ^7\Sigma^+$ states of CrH and MnH are in the Hund case (b) limit, the Zeeman tuning is given by[4]

$$\Delta E^{\text{Zee}} \approx \langle \text{Case } b | \mathbf{H}^{\text{Zee}}(^{2S+1}\Sigma) | \text{Case } b \rangle = g_J \mu_B B_z M_J$$
$$= g_S \frac{[S(S+1) + J(J+1) - N(N+1)]}{2J(J+1)} \mu_B B_z M_J, \quad (2)$$

where J is the total angular momentum, S is the total electron spin angular momentum, M_J is the projection of the total angular momentum, and B_z is the applied magnetic field. The effective g_J-factor for the lowest energy level of the $X\ ^7\Sigma^+$ state ($N=0$, $J=3$) of MnH and the $X\ ^6\Sigma^+$ state ($N=0$, $J=5/2$) of CrH predicted by Eq. (2) is simply the

electron spin g-factor, g_S (=2.0023), because the electron spin is fully decoupled from the molecular axis in the absence of rotation. In actuality rotation, spin orbit, and magnetic field induced mixing could cause the effective g_J-factors for the $^{(2S+1)}\Sigma$ states of CrH and MnH to significantly deviate from those predicted by Eq. (2). The effective Zeeman Hamiltonian operator used to account for these mixings is[4]

$$\hat{\mathbf{H}}^{\text{Zee}}(\text{eff}) = g_S \mu_B \hat{\mathbf{S}} \cdot \hat{\mathbf{B}} + g_L \mu_B \hat{\mathbf{L}} \cdot \hat{\mathbf{B}} + g_\ell \mu_B (\hat{S}_x \hat{B}_x + \hat{S}_y \hat{B}_y)$$
$$+ g_\ell' \mu_B (e^{-2i\phi} \hat{S}_+ \hat{B}_+ + e^{+2i\phi} \hat{S}_- \hat{B}_-), \quad (3)$$

where $\hat{S}_x$ and $\hat{B}_x$ refer to the x-axis molecule fixed components of the electronic spin angular momentum and magnetic field, respectively, and ϕ is the azimuthal angle of the electronic coordinates. Equation (3) is applicable to all electronic states of linear molecules. Precise modeling of the Zeeman effect requires an experimental determination of the g_S and g_ℓ parameters for $^{(2S+1)}\Sigma$ states and of the g_L, g_S, g_ℓ', and g_ℓ parameters for all other electronic states. An analysis of the gas-phase laser magnetic resonance spectrum of the $X\ ^6\Sigma^+$ state of CrH (Ref. 5) determined values for g_S and g_ℓ of 2.001 663(39) and $-4.201(50) \times 10^{-3}$, respectively. An analysis of the matrix isolation electron spin resonance spectrum for the $X\ ^7\Sigma^+$ states of MnH (Ref. 6) determined values for g_S and g_ℓ of 2.002(3) and $-1.8(3) \times 10^{-3}$, respectively. Thus the ($N=0$, $J=3$) $X\ ^7\Sigma^+$ state of MnH and the ($N=0$, $J=5/2$) $X\ ^6\Sigma^+$ state of CrH are not severely mixed, and the magnetic tuning of both states can be fairly accurately modeled using the simple expression of Eq. (2).

Although magnetic trapping involves ground state molecules, an analysis of the Zeeman effect in excited electronic states is also required because monitoring the spatial and temporal molecular concentrations in the magnetic traps is most readily performed using optical spectroscopy.[2] An *a priori* prediction of the magnetic tuning of excited electronic states is typically much less reliable than that of

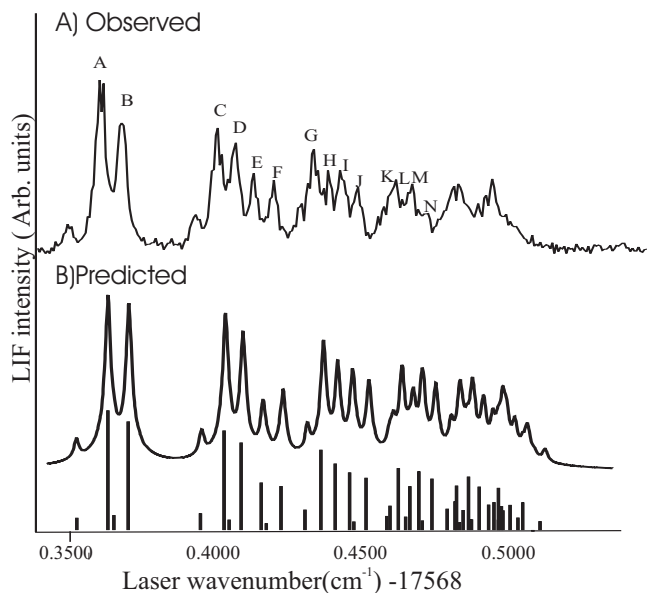a)Telephone: (480) 965-3265. Electronic mail: tsteimle@asu.edu.

FIG. 1. The (a) observed and (b) calculated $P_1(0)$ line ($\nu = 17\,568.35$ cm^{-1}) of the $A\ ^7\Pi_{-2} - X\ ^7\Sigma^+$ (0,0) band of MnH, recorded under field-free conditions. There are a total of 43 transitions; the 14 most intense features are labeled and assigned in Fig. 2.

FIG. 2. The predicted field-free energy levels associated with the $P_1(0)$ line ($\nu = 17\,568.35$ cm^{-1}) of the $A\ ^7\Pi_{-2} - X\ ^7\Sigma^+$ (0,0) band of MnH. The 14 strongest transitions of Fig. 1 are indicated. The energy scale for the $A\ ^7\Pi$ state has been expanded by a factor of 4 relative to that of the $X\ ^7\Sigma^+$ state.

ground states due to the increased density of states. To support experiments aimed at buffer gas cooling and magnetic trapping of CrH, we recently reported on the analysis of the optical Zeeman effect in the $A\ ^6\Sigma^+ - X\ ^6\Sigma^+$ (1,0) and $A\ ^6\Sigma^+ - X\ ^6\Sigma^+$ (0,0) bands.[7] It was observed that the tuning of the $N=0$ and 1 rotational levels in the $A\ ^6\Sigma^+$ ($v=1$) vibronic level was not predictable from Eq. (2) due to perturbations involving the $a\ ^4\Sigma^+$ state. Here we report on the optical Zeeman effect in the $A\ ^7\Pi - X\ ^7\Sigma^+$ (0,0) band of MnH. If it is assumed that the $A\ ^7\Pi$ state is in the Hund case (a) limit and that there is no severe vibronic mixing, then the Zeeman tuning, ΔE^{Zee}, will be simply given by[4]

$$\Delta E^{\mathrm{Zee}} = \mu_B B M_J \Omega [g_L \Lambda + g_S \Sigma]/[J(J+1)] = g_J \mu_B B M_J,$$
(4)

with g_L and g_S having the values of 1 and 2.0023. In Eq. (4), Λ and Σ are the projections of the electronic orbital and spin angular momenta on the internuclear axis and $\Omega = \Lambda + \Sigma$.

The field-free optical spectrum of the $A\ ^7\Pi - X\ ^7\Sigma^+$ (0,0) band is now well characterized as a result of the analysis of the Doppler limited laser induced fluorescence (LIF) spectrum,[8] the sub-Doppler intermodulated fluorescence spectrum,[9] and the supersonic molecular beam LIF spectrum.[10] There is a total of 147 allowed ($\Delta J = 0, \pm 1$) rotational branches and, in addition, many more weak branches associated with $\Delta J = \pm 2$ and ± 3 transitions that gain intensity due to large ^{55}Mn ($I=5/2$) magnetic-hyperfine-induced mixing of spin components within a given low rotational level of the $X\ ^7\Sigma^+$ state. Density functional theory[11,12] and *ab initio*[13] calculations, which predict the magnetic g-factors for ground state MnH in agreement with the ESR results, have been performed. There are no previous measurements or theoretical predictions of the g-factors for the $A\ ^7\Pi$ state.
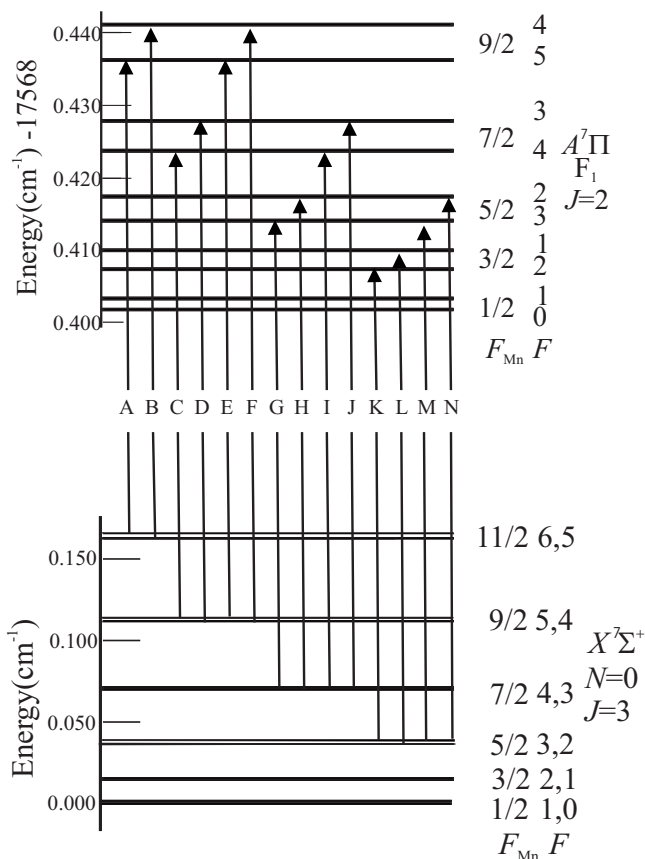
II. EXPERIMENTAL

The molecular beam apparatus has been described previously in the report on the analysis of the field-free LIF spectrum of a MnH molecular beam sample.[10] In the current study precise measurement of the magnetically induced wavelength shifts of the spectral features was achieved by simultaneous recording of the transmission of two confocal etalons with the LIF signal. One etalon, 10 cm in length and thoroughly described in Ref. 14, was thermally stabilized, evacuated, and actively controlled by monitoring the transmission of a frequency stabilized He–Ne laser. The free spectral range (fsr) of the locked etalon was determined to be 749.14 ± 0.01 MHz. A second, unstabilized, 1 m confocal etalon (fsr$=75 \pm 1$ MHz) was used to extrapolate between transmission peaks of the 10 cm, stabilized, confocal etalon.

Static homogeneous magnetic fields approaching 110 mT were generated using a pair of Helmholtz coils with ferromagnetic poles through which 12 mm holes were drilled to allow for the passage of the molecular beam as previously described.[7] Fields up to approximately 370 mT were obtained by adding rare earth cylindrical magnets to the ferromagnetic poles. The field was calibrated using a commercial Gauss meter. A polarization rotator and a polarizing filter were used to orient the electric field vector of the linearly polarized laser radiation either parallel or perpendicular to the static magnetic field, resulting in $\Delta M_J = 0$ or $\Delta M_J = \pm 1$ selection rules, respectively.
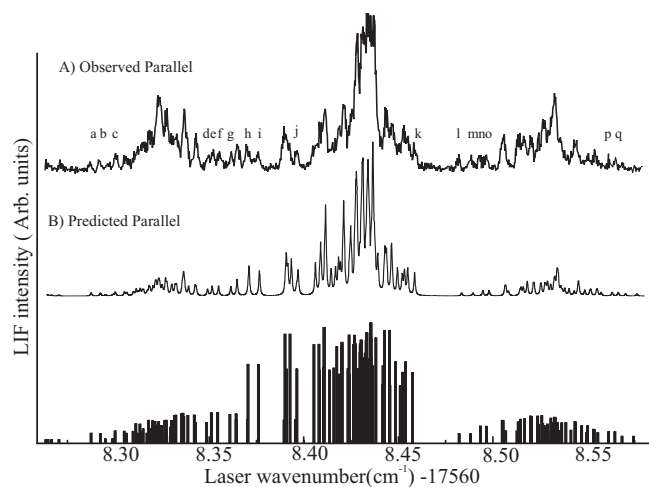
FIG. 3. The observed (upper trace) and predicted (lower traces) $P_1(0)$ line ($\nu=17\,568.35$ cm^{-1}) of the $A\,^7\Pi_{-2}-X\,^7\Sigma^+$ band in the presence of a 102.6 mT applied magnetic field parallel to the electric field of the laser ($\Delta M_F=0$). The Zeeman shifts of the features marked a–q were precisely measured and used in the determination of the g-factors.

III. OBSERVATIONS

A major objective is to determine the Zeeman tuning of intense, unblended optical lines in the $A\,^7\Pi-X\,^7\Sigma^+$ (0,0) band that can be used for diagnostics in helium buffer gas cooling and magnetic trapping experiments where the temperature is less than 1 K.[2] Thus the Zeeman tuning of optical spectral features originating from the lowest rotational level in the electronic ground state ($N''=0$, $J''=3$) is required. It was previously determined from the analysis of the field-free spectrum[10] that the $P_1(0)$ ($\nu=17\,568.35$ cm^{-1}) line was most appropriate because it is relatively intense and unblended. Here the labeling scheme of $\Delta J_{F'}(N'')$ is used, where $F'(=F'')$ is the spin component for the $A\,^7\Pi$ state ($F'=1,2,...,7$ for the $A\,^7\Pi_{-2}$, $A\,^7\Pi_{-1}$, …, $A\,^7\Pi_4$ spin-orbit split components) and F'' is the spin component for the $X\,^7\Sigma^+$ state ($F''=1,2,3,...,7$ for the $J''=N''+3$, $N''+2$, …, $N''-3$ levels). The observed and predicted field-free spectra
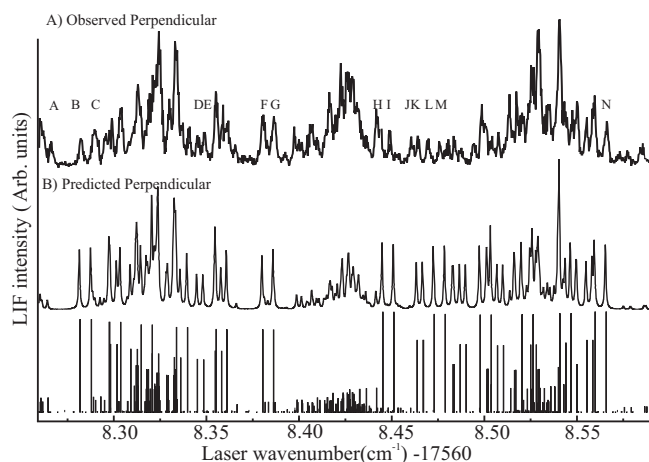

FIG. 4. The observed (upper trace) and predicted (lower traces) $P_1(0)$ line ($\nu=17\,568.35$ cm^{-1}) of the $A\,^7\Pi_{-2}-X\,^7\Sigma^+$ band in the presence of a 102.6 mT applied magnetic field perpendicular to the electric field of the laser ($\Delta M_F=\pm 1$). The Zeeman shift of the features marked A–N were precisely measured and used in the determination of the g-factors.
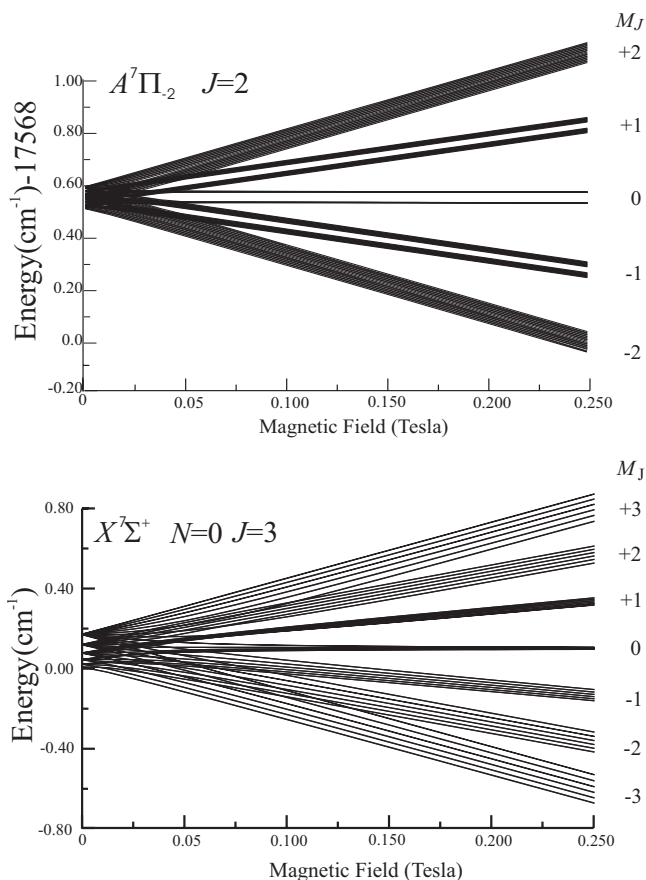

FIG. 5. The predicted energy levels associated with the $P_1(0)$ line ($\nu=17\,568.35$ cm^{-1}) of the $A\,^7\Pi_{-2}-X\,^7\Sigma^+$ (0,0) band of MnH as a function of applied magnetic field. The nuclear spin rapidly decouples from the molecular axis, and the approximately good quantum numbers are M_J, M_I(H), and M_I(Mn).

of the $P_1(0)$ feature are presented in Fig. 1, and the associated energy levels are presented in Fig. 2. The spectrum and energy levels are complicated because of the ^{55}Mn($I=5/2$) and H($I=1/2$) magnetic hyperfine interaction. The H($I=1/2$) interaction is small relative to that of ^{55}Mn($I=5/2$) in the $N''=0$ level of the $X\,^7\Sigma^+$ state, and the energy level pattern consists of six pairs of closely spaced levels associated with the Clebsch–Gordan series of coupling $J=3$ with $I=5/2$. In the excited $A\,^7\Pi_{-2}(F_1)$ state, however, the H($I=1/2$) splitting is only slightly smaller than that due to the ^{55}Mn($I=5/2$) interaction, and the pattern consists of five ($=2J+1$) widely spaced pairs of levels associated with the Clebsch–Gordan series of coupling $J=2$ with $I=5/2$. In both the $A\,^7\Pi_{-2}(F_1)$ and $X\,^7\Sigma^+$ states, the intermediate quantum number of F_{Mn} [$\mathbf{F}_{Mn}=\mathbf{J}+\mathbf{I}$(Mn)] is a useful designation. The 14 most intense features associated with the $P_1(0)$ transition are indicated (labeled A–N) in Figs. 1 and 2. The two most intense features (A and B) are associated with $F''_{Mn}=11/2$ and correspond to the $\Delta J=\Delta F_{Mn}=-1$ transitions. There are a total of 43 allowed field-free transitions.

The observed (upper trace) and predicted (lower traces) spectra of the $P_1(0)$ line recorded in the presence of a 102.6 mT applied magnetic field parallel to the electric field of the laser ($\Delta M_F=0$) are presented in Fig. 3 and with the magnetic field perpendicular to the electric field of the laser
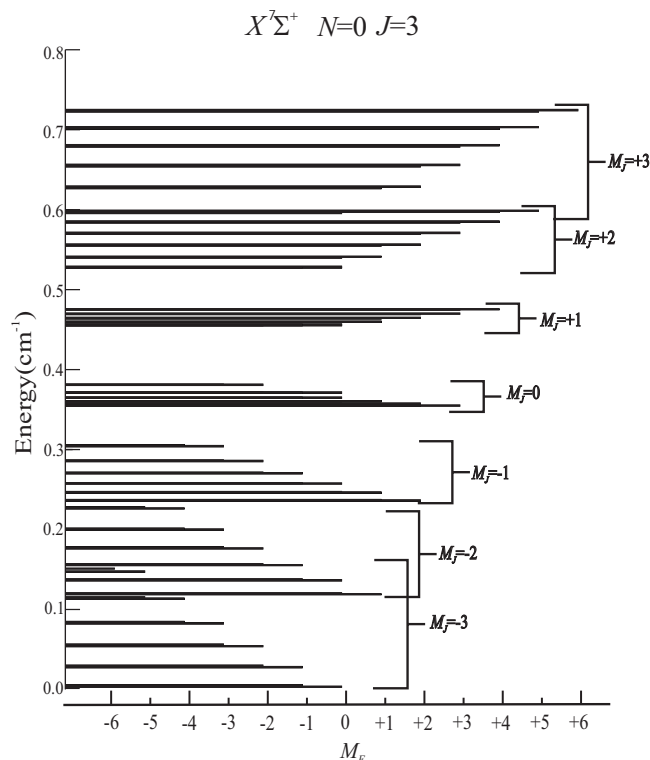
$X\,^7\Sigma^+$ $N=0$ $J=3$

FIG. 6. The predicted components of the $N=0$, $J=3$ rotational level of the $X\,^7\Sigma^+$ ($v=0$) state at 102.6 mT. There are seven ($=2J+1$) groups of 12 levels $[=(2I(^{55}\text{Mn})+1)\times(2I(\text{H})+1)]$. Each group of 12 levels consists of six $[=2I(^{55}\text{Mn})+1]$ pairs exemplifying the approximate goodness of the M_J, $M_I(\text{H})$, and $M_I(^{55}\text{Mn})$ quantum numbers used to designate the transitions in Table I. The M_F quantum number is given by the length of the line.

FIG. 7. The predicted energy levels of the $J=2$ rotational level (F_1-spin component) of the $A\,^7\Pi_{-2}(v=0)$ state at 1026 G. There are five ($=2J+1$) groups of 12 levels $[=(2I(^{55}\text{Mn})+1)\times(2I(\text{H})+1)]$. Each group of 12 levels consists of six $[=2I(^{55}\text{Mn})+1]$ pairs exemplifying the approximate goodness of the M_J, $M_I(\text{H})$, and $M_I(^{55}\text{Mn})$ quantum numbers used to designate the transitions in Table I. The M_F quantum number is given by the length of the line.
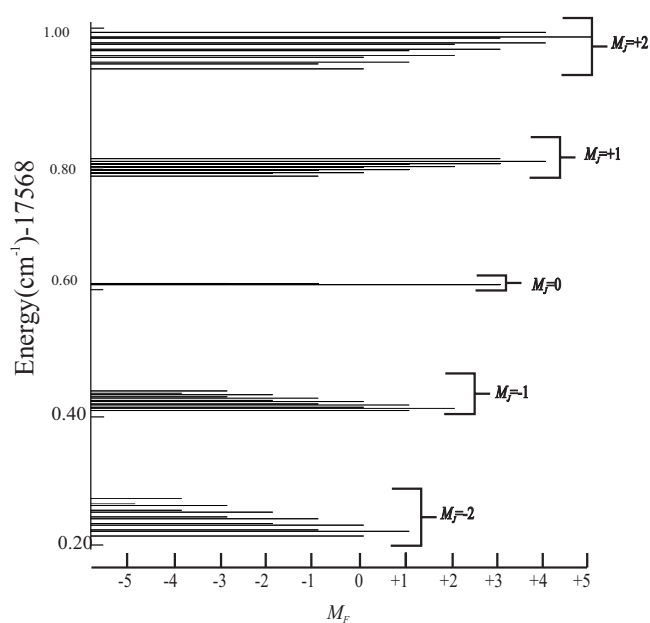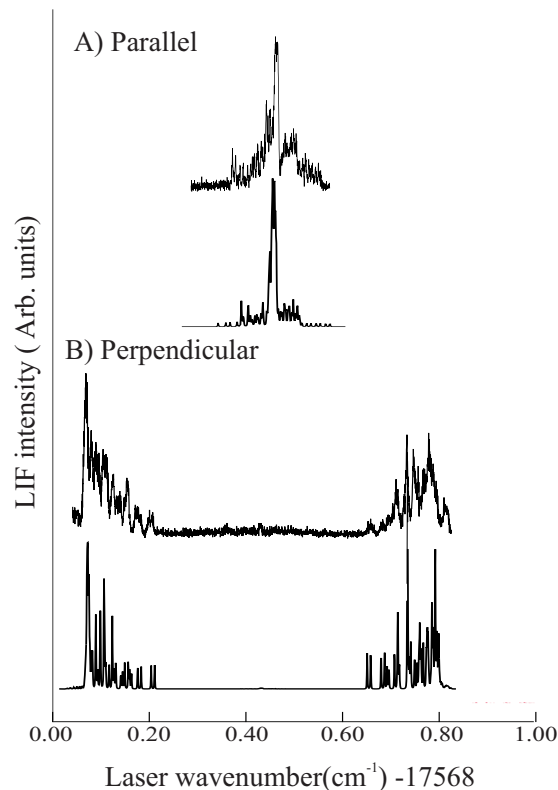

FIG. 8. (Color online) The observed and predicted $P_1(0)$ line ($\nu=17\,568.35$ cm^{-1}) of the $A\,^7\Pi_{-2}-X\,^7\Sigma^+$ band in the presence of a 362.0 mT applied magnetic field that is either parallel ($\Delta M_F=0$) (upper traces) or perpendicular ($\Delta M_F=\pm 1$) (lower traces) to the electric field of the laser.

($\Delta M_F=\pm 1$) in Fig. 4. There are a total of 415 and 671 transitions for the parallel and perpendicular spectra, respectively. For illustrative purposes, the predicted spectra in the center traces of Figs. 3 and 4 were produced using a Lorentzian line shape with a full width at half maximum of 20 MHz, which is slightly less than the observed linewidth of approximately 35 MHz. The energy level pattern associated with the $P_1(0)$ transition as a function of applied magnetic field is presented in Fig. 5. At low fields the energy level pattern is very complex because the $^{55}\text{Mn}(I=5/2)$ and H($I=1/2$) nuclear spins rapidly decouple from the molecular frame upon application of the magnetic field. At moderate fields the energy pattern becomes that expected when the approximately good quantum numbers become M_J, $M_I(\text{Mn})$, and $M_I(\text{H})$. The low and high wavenumber groups of lines in the perpendicular spectrum (Fig. 4) are associated with $\Delta M_J=+1$ and $\Delta M_J=-1$ transitions, respectively. The weak group of essentially unshifted lines in Fig. 4 is associated with the $\Delta M_J=0$ transitions, which in the high-field limit have zero transition probability. The energy level patterns for the $X\,^7\Sigma^+(v=0)$ and $A\,^7\Pi(v=0)$ states at 102.6 mT are illustrated in Figs. 6 and 7, respectively. The pattern of seven ($=2J''+1$; $J''=3$, $X\,^7\Sigma^+$) or five ($=2J'+1$; $J'=2$, $A\,^7\Pi$) groups of six ($=2I+1$; $I(\text{Mn})=5/2$) closely spaced doublets ($=2I+1$; $I(\text{H})=1/2$) is evident. The observed and predicted spectra of the $P_1(0)$ line recorded in the presence of a 306.2 mT applied magnetic field with parallel orientation ($\Delta M_F=0$) (upper trace) and perpendicular orientation ($\Delta M_F=\pm 1$) are presented in Fig. 8. The $\Delta M_J\neq\Delta M_F$ tran-

TABLE I. The Zeeman shifts of the $P_1(0)$ line ($\nu = 17\,568.35$ cm^{-1}) of the $A\,^7\Pi_{-2}$–$X\,^7\Sigma^+$ (0,0) band of manganese monohydride, MnH, recorded at a field of 1026 G. The values in the last two columns are given in MHz (standard deviation of fit: 39 MHz).

Line[a]	M_J'',M_{F_1}'',M_F''	M_J',M_{F_1}',M_F'	F_1'',F''	F_1',F'	Observed	Difference
a	$-1,-4.5,-4$	$-2,-4.5,-4$	5.5,6	4.5,4	-2053	-2
b	$-1,-3.5,-3$	$-2,-3.5,-3$	5.5,5	4.5,4	-1960	4
c	$-1,-2.5,-3$	$-2,-2.5,-3$	4.5,5	3.5,4	-3337	-12
d	$+3,+2.5,+2$	$+2,+2.5,+2$	5.5,5	4.5,4	-739	-7
e	$+1,+0.5,+1$	$+1,+0.5,+1$	4.5,4	3.5,3	-1720	-40
f	$+1,+0.5,0$	$+1,+0.5,0$	5.5,5	3.5,3	-201	-29
g	$+1,-0.5,0$	$+1,-0.5,0$	4.5,5	3.5,4	-1400	-68
h	$-2,-4.5,-5$	$-2,-4.5,-5$	5.5,5	4.5,5	-36	-58
i	$-2,-4.5,-4$	$-2,-4.5,-4$	5.5,5	4.5,5	113	-71
j	$-2,-3.5,-3$	$-2,-3.5,-3$	4.5,4	3.5,3	-473	5
k	$+2,-0.5,-1$	$+2,-0.5,-1$	5.5,6	4.5,4	2563	-47
l	$-3,-4.5,-5$	$-2,-4.5,-5$	4.5,5	4.5,5	1913	-4
m	$-3,-4.5,-4$	$-2,-4.5,-4$	4.5,4	4.5,5	2060	16
n	$-2,-3.5,-4$	$-1,-3.5,-4$	4.5,5	4.5,4	2045	-76
o	$-2,-3.5,-3$	$-1,-3.5,-3$	4.5,4	4.5,5	2307	-6
p	$-2,+0.5,0$	$-1,+0.5,0$	0.5,1	1.5,1	1712	-31
q	$-2,+0.5,+1$	$-1,+0.5,+1$	0.5,1	1.5,2	1888	-30
A	$+3,1.5,+1$	$+1,+0.5,0$	5.5,6	3.5,4	-2632	-29
B	$+3,+5.5+6$	$+2,+4.5,+5$	5.5,6	4.5,5	-2455	-14
C	$+3,+5.5+5$	$+2,+4.5,+4$	5.5,6	4.5,5	-2306	-47
D	$+1,0.5,+1$	$+1,-0.5,0$	4.5,4	3.5,4	-1754	-44
E	$+1,0.5,0$	$+1,-0.5,-1$	5.5,5	3.5,3	-304	-50
F	$+3,0.5,+1$	$+2,-0.5,0$	5.5,6	4.5,5	480	-50
G	$+3,0.5,0$	$+2,-0.5,-1$	5.5,6	4.5,4	500	-62
H	$-3-5.5,-6$	$-2,-4.5,-5$	5.5,6	4.5,5	2423	-11
I	$-3-5.5,-5$	$-2,-4.5-4$	4.5,5	3.5,4	1445	-5
J	$-2,-4.5,-5$	$-1,-3.5,-4$	5.5,6	4.5,4	2838	-20
K	$-2,-4.5,-4$	$-1,-3.5,-3$	5.5,6	4.5,5	3368	-41
L	$-3,-4.5,-5$	$-2,-3.5-4$	5.5,5	3.5,4	3538	-42
M	$-3,-4.5,-4$	$-2,-3.5,-3$	4.5,4	3.5,4	2201	-31
N	$-3,-0.5,0$	$-2,0.5,+1$	0.5,0	0.5,1	2064	-46

[a]See Figs. 3 and 4.

sitions are greatly reduced in intensity compared to the spectra shown in Figs. 4 and 5.

The features marked a–q in Fig. 3 and A–N in Fig. 4 were identified as minimally blended and were used in the analysis (see below). The wavenumber shift of these features from the corresponding field-free transition were precisely measured and are listed in Table I along with the quantum number assignment. In some cases the Zeeman spectral feature extrapolates to a field-free transition that has zero intensity (i.e., a transition for which $|\Delta F| > 1$). In these cases the field-free transition wavelength was established by adding or subtracting the predicted field-free hyperfine splitting in the $X\,^7\Sigma^+$ state required to coincide with the nearest allowed (i.e., $|\Delta F| \leq 1$) transition.

IV. ANALYSIS

The effective Hamiltonian operator used to model the field-free energies of the $A\,^7\Pi$ and $X\,^7\Sigma^+$ states has been described previously in Ref. 10. The matrix representation of the effective Hamiltonian operator was constructed using a Hund case $(a_{\beta J})$ nonparity basis set, $\Psi = |n\Lambda; S\Sigma; J\Omega I_1 F_1 I_2 F M_F\rangle$, and numerically diagonalized to produce the eigenvalues and eigenvectors. Here I_1 and I_2

refer to the ^{55}Mn($I=5/2$) and proton ($I=1/2$) nuclear spins, respectively. For the $A\,^7\Pi$ state the dimension for the representation of the field-free energies is $168(=2\times(2S+1) \times(2I_1+1)\times(2I_2+1))$ and that for the $X\,^7\Sigma^+$ state is 84. The field-free parameters are given in Ref. 10.

The effects of the static magnetic field on the energy levels and wave functions of the $A\,^7\Pi$ and $X\,^7\Sigma^+$ states were modeled by inclusion of the Zeeman Hamiltonian operator given in Eq. (3). The matrix representation of the Zeeman Hamiltonian operator is diagonal in M_F, the projection of total angular momentum, but of infinite dimension. The energies of the levels associated with the $P_1(0)$ line were modeled to a level of accuracy of the experiment (<20 MHz) by truncating the matrix representation to include $F=0$ to $F=6$ for the $X\,^7\Sigma^+$ state and $F=0$ to $F=5$ for the $A\,^7\Pi$ state. In the $X\,^7\Sigma^+$ state this accounts for all the interactions among the field-free energy levels associated with $N=0$, and in the $A\,^7\Pi$ state it accounts for all the interaction $J=2$ levels of the F_1-spin component. Test calculations were performed in a basis set expanded to include $F=0$ to $F=9$ in both states, and the effects at 306.2 mT were less than 5 MHz.

Modeling the spectra was performed by generating the transition moment for each spectral feature by cross multi-

plication of a Hund case $(a_{\beta J})$ electric-dipole transition moment matrix for the $A\,^7\Pi - X\,^7\Sigma^+$ band system with the Hund case $(a_{\beta J})$ eigenvectors for the $X\,^7\Sigma^+$ and $A\,^7\Pi$ states. The transition moment was squared, multiplied by a Boltzmann factor, and a Lorentzian line shape was superimposed on each spectral feature and co-added to produce the predicted spectra.

The 31 shifts in Table I were used as input to a least-squares fitting program. The g_S and g_ℓ for the $X\,^7\Sigma^+$ state were held fixed at values determined from the matrix isolation ESR study,[6] i.e., 2.002(3) and $-1.8(3) \times 10^{-3}$. Fits using various combinations of g_L, g_S, g'_ℓ, and g_ℓ parameters of the $A\,^7\Pi$ state were performed. In the end the anisotropic g-factors, g_ℓ and g'_ℓ, were constrained to zero, g_L was limited to 1.00, and only the g_S parameter was optimized. The electron orbital g-factor, g_L, is expected to differ only slightly from unity owing to small relativistic, diamagnetic, and nonadiabatic effects.[4] The resulting optimized value for g_S is 2.0098(36), where the numbers in parentheses represents a 2σ error estimate. The standard deviation of the fit is 39 MHz, which is commensurate with the measurement uncertainty.

V. DISCUSSION

The optical Zeeman spectrum of the $P_1(0)$ line ($\nu = 17\,568.35$ cm^{-1}) of the $A\,^7\Pi - X\,^7\Sigma^+$ of MnH has been recorded and analyzed. This feature is most convenient for monitoring buffer-gas-cooled and magnetically trapped MnH molecules.[2] The large ^{55}Mn($I = 5/2$) magnetic hyperfine interaction complicates the energy level pattern, particularly at low magnetic field strengths. The anisotropic g-factors, g_ℓ and g'_ℓ, for the $A\,^7\Pi$ state are small and indeterminable at the low magnetic field used. The optimized g_S of 2.0098(36) is slightly larger than the free electron spin g-value. Too little is known about the nature of the low-lying excited states to precisely estimate the anisotropic g-factors, g_ℓ and g'_ℓ. The Curl relationships,[4] $g_\ell = -\gamma/2B$ and $g'_\ell = p/2B$, where γ, p, and B are the spin-rotation, Λ-doubling, and rotational parameters, predict that g_ℓ and g'_ℓ are 1×10^{-3} and 4×10^{-3}, respectively. The Curl relationships are based on a single $^{(2S+1)}\Pi / ^{(2S+1)}\Sigma$ set of interacting states, and the applicability of these approximate relationships to the $A\,^7\Pi$ state is questionable. The Λ-doubling, spin-spin, and spin-rotation parameters, which are reflections of the mixing of the $A\,^7\Pi$ state, are all small. Therefore it may be expected that the effect of the nonadiabatic terms g_ℓ and g'_ℓ will be negligible for the $P_1(0)$ line. Other branch features may be affected due to the rotational dependence of these terms.

The Hund case (b) expression for the effective g-factor given in Eq. (2) predicts a tuning rate of 83.94 MHz/mT for the $N'' = 0$, $J'' = 3$, and $|M_J| = 3$ levels of the $X\,^7\Sigma^+$ state. This

rate is in very close agreement with the 84.07 MHz/mT tuning rate predicted using the more complete modeling as described above because the absence of rotation in the $N'' = 0$ and $J'' = 3$ levels of the $X\,^7\Sigma^+$ state ensures that the electron spin is completely decoupled from the molecular frame. In contrast to the validity of the Hund limiting case tuning rates for the $X\,^7\Sigma^+$ state, the magnetic tuning of the $J' = 2$ and $|M_J| = 2$ levels of the $A\,^7\Pi_{-2}(F_1)$ spin-orbit component is predicted by Eq. (4) to be 46.63 MHz/mT, whereas the more complete modeling predicts, in agreement with the observation, a tuning rate of 60.42 MHz/mT. The large difference between the two predicted tuning rates for the $J' = 2$ and $|M_J| = 2$ levels of the $A\,^7\Pi_{-2}(F_1)$ spin-orbit component is because the $A\,^7\Pi$ state is not near the Hund case (a) limit. The ratio of the spin orbit to rotational parameters, which is a gauge of how strongly the electron spin is coupled to the molecular axis, is only 6.38(=40.5286/6.3483). The tuning of the intense group of spectral features associated with the $N'' = 0$, $J'' = 3$, $|M_J| = 3 \to J = 2$, and $|M_J| = 2$ transitions of the $P_1(0)$ line is ± 23.65 MHz/mT (=84.07−60.42). The information on the Zeeman tuning, as deduced here, can be directly used, for instance, to extract information on the spatial distribution—and thereby the temperature—of a trapped ensemble of MnH molecules in an inhomogeneous magnetic quadrupole trapping field and is required for future studies involving magnetic field manipulation of MnH in general.

[1] J. M. Bakker, M. Stoll, D. R. Weise, O. Vogelsang, G. Meijer, and A. Peters, J. Phys. B **39**, S1111 (2006).
[2] M. Stoll, J. M. Bakker, T. C. Steimle, G. Meijer, and A. Peters, Phys. Rev. A **78**, 032707 (2008).
[3] J. F. Harrison, Chem. Rev. (Washington, D.C.) **100**, 679 (2000).
[4] J. M. Brown and A. Carrington, *Rotational Spectroscopy of Diatomic Molecules* (Cambridge University Press, Cambridge, England, 2003).
[5] S. M. Corkery, J. M. Brown, S. P. Beaton, and K. M. Evenson, J. Mol. Spectrosc. **149**, 257 (1991).
[6] R. J. Van Zee, D. A. Garland, and W. Weltner, Jr., J. Chem. Phys. **85**, 3237 (1986).
[7] J. Chen, J. M. Bakker, A. Peters, M. Stoll, G. Meijer, and T. C. Steimle, Phys. Chem. Chem. Phys. **9**, 949 (2007).
[8] T. D. Varberg, R. W. Field, and A. J. Merer, J. Chem. Phys. **95**, 1563 (1991).
[9] T. D. Varberg, J. A. Gray, R. W. Field, and A. J. Merer, J. Mol. Spectrosc. **156**, 296 (1992).
[10] J. J. Gengler, T. C. Steimle, J. Harrison, and J. M. Brown, J. Mol. Spectrosc. **241**, 192 (2007).
[11] S. Patchkovskii, R. T. Strong, C. J. Pickard, and S. Un, J. Chem. Phys. **122**, 214101 (2005).
[12] S. Patchkovskii and T. Ziegler, J. Phys. Chem. A **105**, 5490 (2001).
[13] M. Munzarova and M. Kaupp, J. Phys. Chem. A **103**, 9966 (1999).
[14] T. C. Steimle, J. J. Gengler, and J. Chen, Can. J. Chem. **82**, 779 (2004).